On Wave Splitting, Source Separation and Echo Removal with Absorbing Boundary Conditions

D. Baffet and M. J. Grote

Departement Mathematik und Informatik
Fachbereich Mathematik
Universität Basel
CH-4051 Basel

Preprint No. 2018-14
September 2018

www.math.unibas.ch

On Wave Splitting, Source Separation and Echo Removal with Absorbing Boundary Conditions

Daniel Baffet, Marcus J. Grote

Department of Mathematics and Computer Science,
University of Basel,
Spiegelgasse 1,
4051 Basel, Switzerland

September 27, 2018

Abstract

Starting from classical absorbing boundary conditions (ABC), we propose a method for the separation of time-dependent wave fields given measurements of the total wave field. The method is local in space and time, deterministic, and makes no prior assumptions on the frequency spectrum and the location of sources or physical boundaries. By using increasingly higher order ABC, the method can be made arbitrarily accurate and is, in that sense, exact. Numerical examples illustrate the usefulness for source separation and echo removal.

1 Introduction

For decades absorbing boundary conditions[1] (ABC) have been used to truncate computational domains [2, 5, 11, 10, 6, 13] for the simulation of time-dependent wave phenomena in unbounded regions. Typically, an ABC consists of a linear partial differential "one-way" operator, B, which eliminates outgoing waves. By imposing the boundary condition

$$B[u] = 0 \tag{1}$$

at the outer artificial boundary, (unphysical) incoming waves are set to zero while outgoing waves remain unaffected. The result is a boundary condition that completes the statement of a well posed initial boundary value problem (IBVP) and allows outgoing waves to leave the computational domain without spurious reflections.

Here we show that one-way operators also permit to split and recover individual wave fields given observations from a time-dependent total wave field, a problem that commonly arises in a variety applications under different disguise. During the collection of marine hydrophone seismic data, for instance, sound wave reflected from the sea floor are recorded by hydrophone streamers towed at a finite depth. After reflection from the (moving) ocean surface, however,

[1] a.k.a. nonreflecting, transparent, outgoing, one-way, etc. boundary conditions

those sound waves travel back generating an (unwanted) echo; the process of removing that ghost signal from the data is also known as "deghosting" [16]. In signal processing, blind source separation uses ray-based statistical tools to detect individual sources [3] or remove noise [1] from their recorded mixture.

When an unknown medium or obstacle is illuminated by an incident probing wave, the scattered data recorded at remote sensors can be used to recover the nature, location or shape of the buried object. While many methods exist to solve such inverse scattering problems, they always assume that the scattered field is readily available by subtraction of the incident wave from total field measurements. Although essential for any subsequent inversion, the extraction of the scattered field certainly becomes nontrivial if the location, spatial distribution or time dependence of the original source are not precisely known or other undesired sources or physical boundaries interfere with the signal. In transcranial ultrasonic imaging [14], for instance, the time signature of the small shock wave induced by cavitation bubbles is never precisely known. Similarly, in photoacoustic imaging [17], the time signature of the laser induced ultrasonic pressure wave generated by the transient thermoelastic expansion of biological tissues is hardly available.

In the presence of two or more obstacles, the inversion from total field measurements is greatly simplified if the multiple scattered fields can be split into individual outgoing components; then, each isolated scattering problem will be smaller in size and less ill-conditioned than their total sum. There is a long history of wave splitting techniques for multiple scattering problems, but mainly in the frequency domain. By combining the inverse Radon approximation with a Galerkin ansatz, Griesmaier, Hanke and Sylvester determine the convex scattering support of individual far-field components separately [7]. For time-dependent source separation, Potthast, Fazi and Nelson recently devised a filter using the point source method via Fourier transform in the frequency domain [15]. Recently, Grote, Kray, Nataf and Assous devised a method to split a time-dependent, scattered, total wave field into its distinct outgoing components induced by separate sources or obstacles [9]. While their approach is purely local in space and time, it still requires deriving a first-order hyperbolic PDE satisfied by each scattered field component on the observational boundary.

Here we propose a different approach for the separation of time-dependent wave fields, which is still local in space and time but does not require deriving any new PDE. In Section 2, we consider a simple generic set-up to illustrate the basic underlying idea. Next, we recall in Section 3 a particular family of one-way operators based on the high-order ABC by Collino [4]. Finally, in Section 4, we illustrate through numerical examples how to apply the our one-way wave splitting approach to source separation and echo removal.

2 Wave splitting

We consider the simple but generic set-up of source separation in free space to present the main idea underlying our approach for wave splitting. Hence, let the total wave field u satisfy the wave equation

$$\frac{\partial^2 u}{\partial t^2} - \Delta u = F(x, y, t) \tag{2}$$

in $\mathbb{R}^2 \times (0, T)$ with homogeneous initial conditions at time $t = 0$. Now, let F be given by

$$F = F_1 + F_2 \tag{3}$$

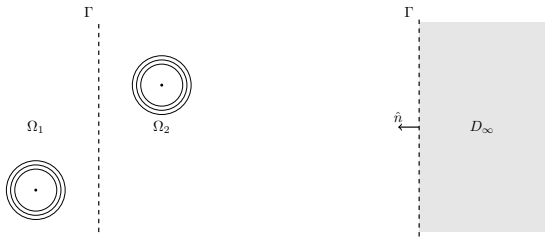

Figure 1: Source separation, generic set-up. Left: unsplit problem posed in $\mathbb{R}^2$; right: setup in D_∞ for the approximation v_1 of u_1

where each F_1 and F_2 is compactly supported in $\Omega_1 = \{x < 0\}$, and $\Omega_2 = \{x > 0\}$, respectively. Then, the wave field u admits the unique (Kirchhoff) decomposition [8]

$$u = u_1 + u_2 \ , \tag{4}$$

where u_1 and u_2 each solve (2) in $\mathbb{R}^2 \times (0,T)$ with $F = F_1$ and $F = F_2$, respectively. From Ω_1, the wave field u_1 thus appears purely outgoing as it crosses the separating artificial boundary Γ (y-axis) at $x = 0$, and vice-versa for u_2.

More generally, when Ω includes nonzero initial conditions, obstacles or inhomogeneities, all compactly supported outside some neighborhood of Γ, the same decomposition (4) still holds in that neighborhood. Each wave field u_i then solves the homogeneous wave equation with zero initial conditions, no obstacles and constant wave speed outside Ω_i, $i = 1, 2$; therefore, u_i is entirely determined inside Ω_j, $j \neq i$, by the boundary condition imposed on Γ.

Given the time-dependent total wave field u and its normal derivative $\partial u/\partial n$ on Γ, we wish to recover u_1 and u_2 on Γ for all t. As seen from Γ, u_1 is purely rightward moving whereas u_2 is purely leftward moving; therefore, we may use one-way operators to distinguish between them.

Let B be a one-way operator such that $B[u_2] = 0$ on Γ and the corresponding IBVP in Ω_2 is well-posed. Applying B to u on Γ then yields

$$B[u_1] = B[u_1] + B[u_2] = B[u]. \tag{5}$$

Assuming that $B[u]$ can be computed from the measured total field u, (5) clearly yields an inhomogeneous boundary condition for u_1. Still, it is by no means obvious how to reconstruct u_1 itself from (5), as it involves not only time and tangential but also normal derivatives of u_1 at Γ. For Γ a circle, (5) can be used to derive a hyperbolic partial differential equation for u_1, which involves only time and tangential derivatives and thus can be solved on Γ [9].

Instead, we note that u_1 is the unique solution of the IBVP in $D_\infty = \{x > 0\}$:

$$\frac{\partial^2 v}{\partial t^2} - \Delta v = 0 \qquad \text{in } D_\infty \times (0,T) \tag{6a}$$

$$B[v] = g(y,t) \qquad \text{on } \Gamma \times (0,T) \tag{6b}$$

$$v(0) = 0 \qquad \text{in } D_\infty \ , \tag{6c}$$

with $g = B[u]$, which is well-posed by assumption. Although here D_∞ coincides with Ω_2, this is not true in general – see Section 4.2, for instance. To recover u_1, we simply solve numerically the IBVP (6) in D_∞. In fact, when u_1 is only required on Γ, we may simply restrict the computation to the vicinity of Γ. Clearly, once u_1 is known we immediately recover $u_2 = u - u_1$.

In practice, the ABC (1) does not eliminate all rightward moving waves. Then $B[u_2]$, albeit small, is not identically zero and the first equality in (5) holds only approximately. Nevertheless, we may still solve (6) with $g = B[u]$, thereby introducing a perturbation, $B[u_2]$, into g. Since (6) is well-posed, that perturbation will only result in a small error in the reconstruction

of u_1. Depending on the application considered, that error may or may not be significant. By choosing a sufficiently accurate one-way operator B, however, that error can always be made arbitrarily small.

3 High-order ABC

To recover u_1 from u on Γ, we require a one-way operator B that discriminates between incoming and outgoing waves and also yields a well-posed IBVP (6) in D_∞. Here, we consider the high-order ABC by Collino [4, 6] and let B equal the corresponding P-th order one-way operator:

$$B[w] = \left(\frac{\partial w}{\partial t} - \frac{\partial w}{\partial x}\right)\bigg|_\Gamma - \sum_{p=1}^{P} b_p \frac{\partial \psi_p}{\partial t} \tag{7a}$$

where $v|_\Gamma$ denotes the restriction of v to Γ and each auxiliary function $\psi_p = \psi_p(y,t)$, $p = 1,\ldots,P$, solves the following initial value problem:

$$\begin{aligned} &\frac{\partial^2 \psi_p}{\partial t^2} - a_p \frac{\partial^2 \psi_p}{\partial y^2} = \frac{\partial^2 w}{\partial y^2}(x,y,t)\ , \quad (x,y) \in \Gamma\ , \\ &\psi_p(y,0) = \frac{\partial \psi_p}{\partial t}(y,0) = 0\ . \end{aligned} \tag{7b}$$

Note that (7b) only involves tangential and time derivatives of ψ_p, which are only defined and computed on Γ.

For well-posedness [18], the parameters $a_1,\ldots,a_P$ and $b_1,\ldots,b_P$ must satisfy $0 < a_p < 1$ and $b_p > 0$ for $p = 1,\ldots,P$, $a_p \neq a_k$ for $p \neq k$, and

$$\sum_{p=1}^{P} \frac{b_p}{1-a_p} < 1\ . \tag{8}$$

Following [6], we choose

$$a_p = \cos^2\left(\frac{\pi p}{2P+1}\right) \tag{9a}$$

$$b_p = \frac{2}{2P+1}\sin^2\left(\frac{\pi p}{2P+1}\right)\ . \tag{9b}$$

Note that parameter values may be adapted to any particular problem. The ABC becomes increasingly accurate with increasing P; hence, it is exact in the sense that we can always choose P sufficiently large to reduce the error in the boundary condition below a prescribed error tolerance (without moving Γ any farther).

For computations, we truncate D_∞ by a vertical perfectly matched layer (PML) in the x direction [12]. In principle, the truncated domain (excluding the PML) can be arbitrarily narrow and even consist only of a fixed number of mesh points in width; thus, its width may even shrink with decreasing mesh size h.

4 Numerical examples

Here we consider two distinct applications of wave splitting: source separation and echo removal. All computations are performed on an equidistant Cartesian mesh with standard second-order finite differences in space and time. We let T denote the final time, $h > 0$ the mesh size and $\kappa > 0$ the time step. The relative global error in the reconstruction u_1^h of u_1 at Γ is measured as

$$E = \frac{\|u_1^h - u_1\|_{\Gamma,T}}{\|u_1\|_{\Gamma,T}}\ , \tag{10}$$

where

$$\|w\|_{\Gamma,T} = \max_{n,j} \left|w|_\Gamma\,(y_j,t_n)\right|. \tag{11}$$

for any grid function w evaluated at time $t_n = n\,\kappa$, $n \geq 0$.

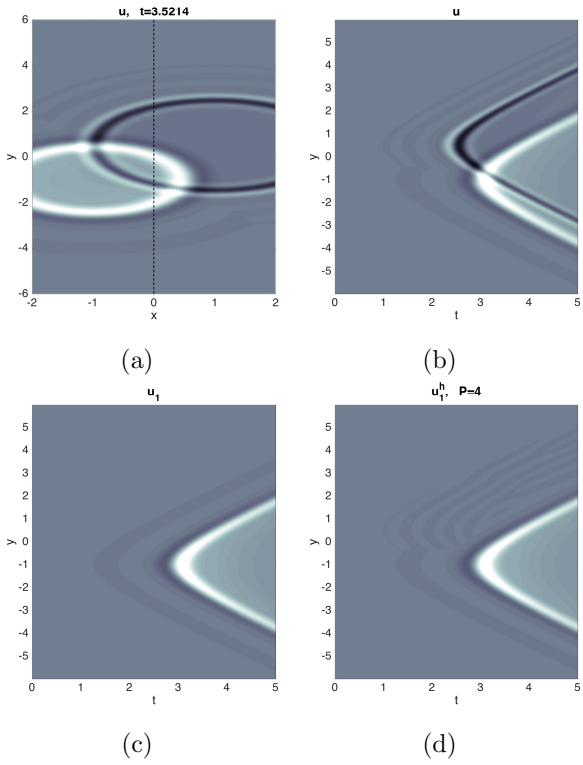

(a) (b) (c) (d)

Figure 2: Source separation. (a) Snapshot of u at $t \approx 3.5$; the measurement surface Γ is marked by a dashed line, (b) the space-time data u on Γ, (c) the reference solution u_1 (d) the split data u_1^h obtained with $P = 4$

4.1 Source separation

First, we consider the generic set-up from Section 2 and let the total wave field u and its normal derivative $\partial u/\partial x$, both recorded at Γ, consist of two outward propagating circular waves $u = u_1 + u_2$ in free space, each u_i originating from its respective half-space Ω_i on either side of the y-axis. Following the approach described in Section 2, we shall now reconstruct u_1, given the time history of the total wave field u, and its normal derivative $\partial u/\partial x$ on Γ. To do so, we solve the IBVP (6) with $g = B[u]$ computed at Γ. The infinite domain D_∞ is truncated at $x = 5h$, that is at a distance of five mesh points from Γ, beyond which a PML is added to absorb outward going waves. We set $h = 10^{-2}$ and $\kappa > 0$ according to the CFL stability condition of the leap-frog method.

Figure 2a shows a snapshot of the total field u at $t \approx 3.5$ whereas Figure 2b displays the space-time data on Γ used for the reconstruction. In particular, we observe the emergence of two space-time cones as the leftward and rightward moving wave fronts cross Γ. The numerical solution, u_1^h, of the IBVP (6) is shown in Figure 2d and compares remarkably well with the reference solution, u_1, shown in Figure 2c. In fact, u_1 and u_1^h essentially coincide, as shown in the left frame of Figure 3 where we compare their time evolution at a fixed location $(x, y) = (0, 0)$. In the right frame of Figure 3, we observe that the relative space-time global error E, given by (10), decays exponentially with P until it saturates at the level of the discretization error.

We recall that our wave-splitting approach makes no use of the locations or space-time dependence of the sources. In fact, it is independent of the sources generating the waves and would remain identical in the presence of obstacles or inhomogeneities.

4.2 Echo removal

Next, we show how to remove an (undesired) echo due to a physical boundary (wall, ocean surface, etc.) from the total wave field observed again on the y-axis Γ at $x = 0$. The incident wave field u_1 originates from the left half-space $\Omega_1 = \{x < 0\}$. After crossing the observational boundary Γ, the incident signal u_1 enters the

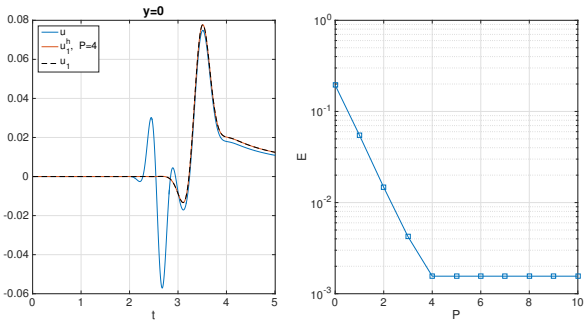

Figure 3: Source separation. Left: the numerical solution u driven by the two sources, the reference solution u_1 and the reconstructed signal u_1^h at $(x, y) = (0, 0)$; right: the relative global error E as a function of P.

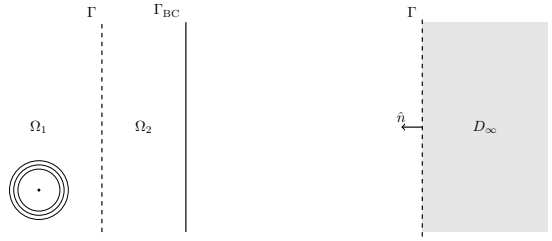

Figure 4: Echo removal, generic setup. Left: unsplit problem posed in $\mathbb{R}^2$; right: setup in D_∞ for the approximation v_1 of u_1

subdomain $\Omega_2 = \{0 < x < b\}$ until it impinges upon the physical boundary $\partial\Omega = \Gamma_{\text{BC}}$, located at $x = b$, where it is reflected; the resulting signal u_2 then propagates back and causes an (undesired) echo in the observations of the total field u at Γ.

Hence, the total wave field u satisfies (2) in $\Omega = (-\infty, b) \times \mathbb{R}$, with $b > 0$ and homogeneous initial conditions at $t = 0$. The source F consists of two point sources located inside Ω_1 and we impose a homogeneous Dirichlet boundary condition $u = 0$ at the physical boundary $\partial\Omega = \Gamma_{\text{BC}}$ located at $x = b$, for simplicity – see Figure 4.

Given measurements of the total field at $\Gamma = \{x = 0\}$, we wish to recover the signal u_1 on Γ from the total field u and thus effectively remove the echo u_2 generated by the physical boundary at $x = b$. To do so, we let $D_\infty = \{x > 0\}$ and consider (6), where B is a Collino operator (7) of order P. Now, we again solve the IBVP (6) for u_2 numerically using the same parameters (mesh size, time-step, etc.) as in Section 2.1.

Figure 5a shows a snapshot of the total field u at $t \approx 3.5$ whereas Figure 5b displays the space-time data on Γ used for the reconstruction. In Fig. 5b, in particular, we see the two space-time cones which correspond to the two point sources located at $(x, y) = (-0.5, 0)$, and $(x, y) = (-0.7, 0.5)$, respectively. Upon comparison of the total field u in Figure 5b with the reference solution u_1 in Figure 5c, we observe how the reflection from the physical right wall propagates back and crosses the incoming signal while causing destructive interference behind the first arrival.

The numerical solution, u_1^h of the IBVP (6) is shown in Figure 5d and compares remarkably well with the reference solution u_1. Again, u_1 and u_1^h essentially coincide, as shown in the left frame of Figure 6 where we compare their time evolution at a fixed location $(x, y) = (0, 0)$. In the right frame of Figure 6, we observe that the relative space-time global error E, given by (10), decays exponentially with P until it saturates at the level of the discretization error.

Again, we emphasize that our wave-splitting approach does not rely on any information from the sources and applies regardless of the type of boundary condition imposed at the (possibly moving) physical boundary $\partial\Omega$. It would also

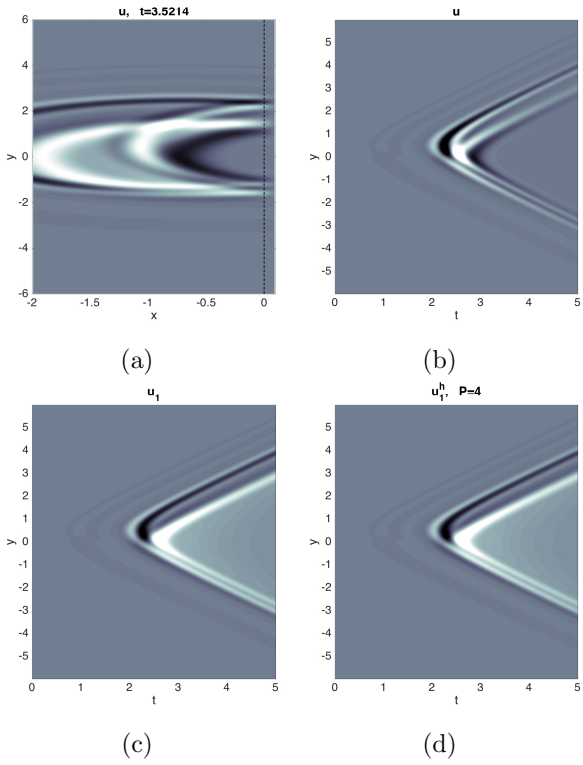

Figure 5: Echo removal. (a) Snapshot of u at $t \approx 3.5$, where Γ is marked by a dashed line, (b) full data u on Γ, (c) reference solution u_1, (d) the recovered u_1^h obtained with $P = 4$.

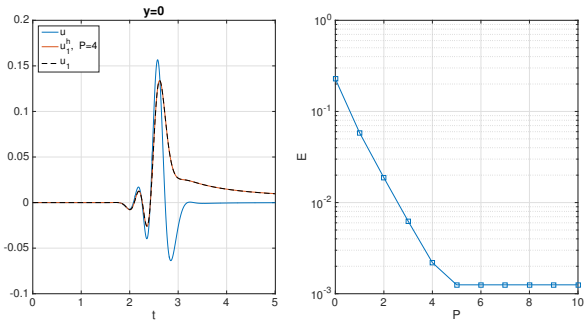

Figure 6: Echo removal. Left: the numerical solution u driven by the two sources, the reference solution u_1 and the reconstructed signal u_1^h at $(x, y) = (0, 0)$; right: the relative global error E as a function of P.

apply in the presence of inhomogeneity or obstacles compactly supported inside Ω_1 or Ω_2.

5 Concluding remarks

Starting from high-order ABC, we have shown how to split a wave field $u = u_1 + u_2$ into individual "one-way" components u_1 and u_2, given observations of the total field u at some recording boundary Γ. Thus, we can separate wave fields originating from different (unknown) sources or remove an unwanted echo in measurements due to a (possibly unknown or moving) physical boundary. Our wave-splitting approach is deterministic and local both in space and time, as it involves no integrals or Fourier transforms. It also makes no prior assumptions on the frequency spectrum or the location of sources or physical boundaries.

To reconstruct u_1, for instance, we first choose a one-way differential operator, B, from a known high-order ABC for which $B[u_2]$ vanishes. Then, we numerically solve the IBVP (6) for u_1 in a computational domain, located on one side of Γ, where we impose an inhomogeneous boundary condition that involves the observations via $B[u]$. The accuracy in the reconstruction of u_1 (or u_2) is determined by the accuracy of the ABC and the numerical discretization error. Both can be made arbitrarily small and hence, in that sense, our approach is exact. As the computational domain along Γ can be arbitrarily narrow, the computational effort for the reconstruction is kept minimal. While we have used the family of high-

order ABCs by Collino [4] here, other ABCs certainly apply, too.

For inverse scattering problems, our approach also permits to extract the scattered field from measurements of the total (physical) wave field, when the incident wave is only partially known, say, when the location or direction but not the time dependence of the source is known. Even in situations of multiple scattering, our approach still permits to split the right- and left-moving components u_1 and u_2 of the total field bouncing back and forth between two obstacles. However, each individual wave field, u_i, will not precisely correspond to the scattered field resulting due to the illumination of a single obstacle, but instead also contain all higher order one-way moving multiple reflections.

References

[1] R. Aichner and H. Buchner and F. Yan and WK̇ellermann: *A real-time blind source separation scheme and its application to reverberant and noisy acoustic environments.*, Signal Processing **86** (2006), pp. 1260–1277.

[2] A. Bayliss and E. Turkel: *Radiation boundary conditions for wave-like equations.* Comm. Pure Appl. Math. **33**, pp. 707–725, 1980

[3] M. Castella, P. Bianchi, A. Chevreuil, J.-C. Pesquet: *A blind source separation framework for detecting CPM sources mixed by a convolutive MIMO filter*, Signal Processing **86** (2006), pp. 1950–1967.

[4] F. Collino, *High Order Absorbing Boundary Conditions for Wave Propagation Models. Straight Line Boundary and Corner Cases*, Proc. 2nd Int. Conf. on Mathematical & Numerical Aspects of Wave Propagation.

[5] B. Engquist and A. J. Majda: *Absorbing boundary conditions for the numerical simulation of waves.* Math. Comp. **31** (139), pp. 629–651, 1977

[6] D. Givoli, *High-Order Local Non-Reflecting Boundary Conditions: A Review*, Wave Motion, 39 (2004), 319-326.

[7] R. Griesmaier, M. Hanke and J. Sylvester, *Far Field Splitting for the Helmholtz Equation*, SIAM J. Numer. Anal. 52 (2014), pp. 343–362.

[8] M. J. Grote, C. Kirsch, *Nonreflecting Boundary Conditions for Time-Dependent Multiple Scattering*, J. Comput. Phys., 221 (2007), 41-62.

[9] M. J. Grote, M. Kray, F. Nataf and FȦssous, *Time-dependent wave splitting and source separation*, J. Comput. Phys., 330 (2017), 981–996.

[10] M. J. Grote: *Local nonreflecting boundary condition for Maxwell's equations.* Comput. Methods Appl. Mech. Engrg. **195**, pp. 3691–3708, 2006

[11] T. Hagstrom and S. I. Hariharan, *A formulation of asymptotic and exact boundary conditions using local operators*, Appl. Numer. Math., **27**, pp. 403–416 (1998).

[12] M. J. Grote, I. Sim, *Perfectly Matched Layer for the Second-Order Wave Equation*, Proceedings of the Ninth International Conference on Numerical Aspects of Wave Propagation (WAVES 2009, Pau, France, 2009), pp. 370–371.

[13] T. Hagstrom, T. Warburton, *Complete Radiation Boundary Conditions: Minimizing the Long Time Error Growth of Local Methods*, SIAM J. Numer. Anal., Vol. 47 (2009), pp. 3678–3704.

[14] M. Pernot, G. Montaldo, M. Tanter, and M. Fink: *Ultrasonic stars for time reversal focusing using induced cavitation bubbles*, Appl. Phys. Lett. 88 (2006), pp. 034102

[15] R. Potthast, F. M. Fazi, and P. A. Nelson: *Source splitting via the point source method*, Inverse Problems 26 (2010), pp. 045002

[16] J. O. A. Robertsson, L. Amundsen: *Wave equation processing using finite-difference propagators, Part 2: Deghosting of marine hydrophone seismic data*, Geophysics, Vol. 79 (2014), pp. T301–T312.

[17] T. Saratoon, T. Tarvainen, B. T. Cox, and S. R. Arridge: *A gradient-based method for quantitative photoacoustic tomography using the radiative transfer equation*, Inverse Problems 29 (2013), pp. 075006

[18] L. N. Trefethen, L. Halpern, *Well-Posedness of One-Way Wave Equations and Absorbing Boundary Conditions*, Math. Comp., Vol. 47 (1986), 421-435.

LATEST PREPRINTS

No.	Author: *Title*
2017-07	**H. Harbrecht and M. Schmidlin** *Multilevel Methods for Uncertainty Quantification of Elliptic PDEs with Random Anisotropic Diffusion*
2017-08	**M. Griebel and H. Harbrecht** *Singular value decomposition versus sparse grids: Refined complexity Estimates*
2017-09	**J. Garcke and I. Kalmykov** *Efficient Higher Order Time Discretization Schemes for Hamilton-Jacobi-Bellman Equations Based on Diagonally Implicit Symplectic Runge-Kutta Methods*
2017-10	**M. J. Grote and U. Nahum** *Adaptive Eigenspace Regularization For Inverse Scattering Problems*
2017-11	**J. Dölz, H. Harbrecht, S. Kurz, S. Schöps and F. Wolf** *A Fast Isogeometric BEM for the Three Dimensional Laplace- and Helmholtz Problems*
2017-12	**P. Zaspel** *Algorithmic patterns for $\mathcal{H}$-matrices on many-core processors*
2017-13	**R. Brügger, R. Croce and H. Harbrecht** *Solving a free boundary problem with non-constant coefficients*
2017-14	**M. Dambrine, H. Harbrecht and B. Puig** *Incorporating knowledge on the measurement noise in electrical impedance tomography*
2017-15	**C. Bürli, H. Harbrecht, P. Odermatt, S. Sayasone and N. Chitnis** *Analysis of Interventions against the Liver Fluke, Opisthorchis viverrini*
2017-16	**D. W. Masser** *Abcological anecdotes*
2017-17	**P. Corvaja, D. W. Masser and U. Zannier** *Torsion hypersurfaces on abelian schemes and Betti coordinates*
2017-18	**F. Caubet, M. Dambrine and H. Harbrecht** *A Newton method for the data completion problem and application to obstacle detection in Electrical Impedance Tomography*
2018-01	**H. Harbrecht and P. Zaspel** *On the algebraic construction of sparse multilevel approximations of elliptic tensor product problems*

LATEST PREPRINTS

No.	Author: *Title*
2018-02	**F. Ghiraldin and X. Lamy** *Optimal Besov differentiability for entropy solutions of the eikonal equation*
2018-03	**H. Harbrecht and M. Schmidlin** *Multilevel quadrature for elliptic problems on random domains by the coupling of FEM and BEM*
2018-04	**M. Bugeanu and H. Harbrecht** *Parametric representation of molecular surfaces*
2018-05	**A. Abdulle, M. J. Grote and O. Jecker** *Finite element heterogeneous multiscale method for Elastic Waves in Heterogeneous Media*
2018-06	**M. J. Grote and J. H. Tang** *On controllability methods for the Helmholtz equation*
2018-07	**H. Harbrecht and M. Moor** *Wavelet boundary element methods — Adaptivity and goal-oriented error estimation*
2018-08	**P. Balazs and H. Harbrecht** *Frames for the solution of operator equations in Hilbert spaces with fixed dual pairing*
2018-09	**R. Brügger, R. Croce and H. Harbrecht** *Solving a Bernoulli type free boundary problem with random diffusion*
2018-10	**J. Dölz, H. Harbrecht and M. D. Multerer** *On the best approximation of the hierarchical matrix product*
2018-11	**H. Harbrecht and P. Zaspel** *A scalable $\mathcal{H}$-matrix approach for the solution of boundary integral equations on multi-GPU clusters*
2018-12	**H. Harbrecht, N. Ilić and M. D. Multerer** *Acoustic scattering in case of random obstacles*
2018-13	**D. H. Baffet, M. J. Grote, S. Imperiale and M. Kachanovska** *Energy decay and stability of a perfectly matched layer for the wave equation*
2018-14	**D. Baffet and M. J. Grote** *On wave splitting, source separation and echo removal with absorbing boundary conditions*